Early dosage compensation of zygotically-expressed genes in *Drosophila melanogaster* is mediated through a post-transcriptional regulatory mechanism

Victoria M. Blake[1,#*], Michael B. Eisen[1,2,3,#]

[1]Department of Molecular and Cell Biology, University of California, Berkeley, California, United States of America

[2]Department of Integrative Biology, University of California, Berkeley, California, United States of America

[3]Howard Hughes Medical Institute, University of California, Berkeley, California, United States of America

[#]Current Address: 151A Koshland Hall, Berkeley, California, 94720, United States of America

[*]Corresponding author

Email: victoriamblake104@gmail.com

Full title: Early Dosage Compensation of zygotically-expressed genes in *Drosophila melanogaster* is mediated through a post-transcriptional regulatory mechanism

Short title: Regulation of RNA abundance of X-linked genes during early embryogenesis in *Drosophila melanogaster*

Funding: This work was funded by a Howard Hughes Medical Institute Investigator award to MBE, and a National Science Foundation Graduate Research Fellowship to VMB. The funders had no role in study design, data collection and analysis, decision to publish, or preparation of the manuscript.

Competing Interests: MBE is a co-founder of PLOS.

Abstract:

Many key regulators of early embryogenesis in *Drosophila melanogaster* are X-linked. However, the canonical, MSL-mediated dosage compensation, which involves hyper-transcription of the genes on the single X chromosome in males, is not active until the post-syncytial stage of development. A separate MSL-independent dosage compensation system active earlier in development has been described, though the mechanism through which the process functions remain unclear. In this study, we quantified transcription in living embryos at single-locus resolution to determine if early dosage compensation of the X-linked genes *buttonhead* and *giant* is sensitive to X

chromosome dose. We found no evidence for a transcriptionally regulated mechanism of early dosage compensation, suggesting that the previously observed compensation of mRNA levels for these genes is achieved via a post-transcriptional regulatory mechanism.

Introduction

In multicellular diploid organisms with chromosomal sex determination, the functional degeneration of sex chromosome specific to the heterogametic sex (the Y in XY systems and W in ZW systems) creates a dosage imbalance for sex-chromosome encoded genes. To mitigate the detrimental impact that this dosage imbalance could have on fitness, a variety of mechanisms have evolved to equalize the abundance of gene products found on only one sex chromosome (typically the X or Z).

In the vinegar fly *Drosophila melanogaster*, which uses an XX/XY sex-determination system, dosage compensation is achieved by upregulating transcription of genes on the male X chromosome (reviewed in Kuroda et al. 2016). Mutations that affect this process are lethal in males (Belote and Lucchesi 1980, Lucchesi and Skripsky 1981, Hilfiker et al. 1997, Meller and Ratner 2002).

All but one of the Male Sex Lethal (MSL) proteins that mediate this process are present in the maternally deposited protein component. Male specificity is achieved through the

activity of the male-specific MSL-2, which directs assembly of the dosage compensation complex to the X chromosome, resulting in acetylation of H4K16 by MOF (Hilfiker et al. 1997, Smith et al. 2000) and a subsequent doubling of transcription from X-linked genes (Smith et al. 2001, Gelbart et al. 2009).

However, an early, MSL-2 independent dosage compensation system acting on *runt* was discovered via genetic experiments (Gergen 1987, Bernstein and Cline 1994) and shown to apply more broadly by direct measurement of mRNA levels in early male and female embryos (Lott et al. 2011). It was hypothesized, based on the enrichment of putative binding sites for the master sex regulator Sxl in the 5' and 3' untranslated regions of X encoded genes, that this system was based on post-transcriptional regulation of mRNA levels (Bernstein & Cline 1994, Lott et al. 2011).

Here we use quantitative live-embryo imaging (Garcia et al. 2013, Bothma et al. 2014) to compare rates of transcription at individual X-linked loci across early development in male and female embryos. Briefly, transcription of a gene tagged with a reporter sequence (MS2 or PP7) forms stem loops that, when bound by a coat protein (MCP or PCP) conjugated to GFP, gives rise to a fluorescent signal. This allows for simultaneous direct quantification via microscopy of transcription rates at individual loci across many nuclei. The ability to quantify transcription rates of candidate genes in embryos of both sexes makes this system uniquely amenable for testing if early dosage compensation is due to increasing the rate of transcription of genes on the male X chromosome.

We focus on four X-linked genes: *giant* (*gt*) and *buttonhead* (*btd*) that had previously been shown to be dosage compensated in the early embryo, and *embryonic lethal abnormal vision* (*elav*) and *bangles and beads* (*bnb*) whose early mRNA levels are dosage sensitive. We found that the early dosage compensation observed for these genes was not due to a doubling of transcription in males, suggesting that this process is likely regulated post-transcriptionally. In addition, we discovered an unreported doubling of the transcription rate in females for *elav*, a gene that is not dosage compensated and has no defined role in sex differentiation.

Materials and Methods:

DNA constructs:

Fly strains were tagged with MS2 or PP7 reporter sequences at the endogenous loci of X-linked genes through CRISPR-Cas9 Homology-Directed Recombination. We used the U6-gRNA protocol from flycrispr.org (Gratz et al. 2016) to clone three guide RNA sequences per gene, targeting a 100 bp region around the start codon, into pCFD5 plasmids (Port and Bullock 2016). For donor plasmids, we inserted a 24X MS2 or PP7 cassette (Garcia et al. 2013, Liu et al. 2020) between 1kb of homology arms for a gene of interest into a pUC19 vector backbone using the NEBuilder HiFi DNA Assembly protocol. We attempted to tag all target genes with both MS2 and PP7, but, due to low editing efficiency and potentially other factors, recovered only one for each gene, as described in text.

Fly line generation:

gRNA, donor, and selection plasmids (for phenotypic screening, Kane et al. 2017) were purified and sent to Rainbow Transgenic Inc. for microinjection into *y2 cho2 v1; Sp/CyO, P{nos-Cas9, y+, v+}2A* embryos.

Full details of construct and sequence information can be found in a public Benchling folder.

Progeny of injected flies with an *ebony* phenotype were molecularly screened by PCR for the insertion of the MS2 or PP7 cassettes at endogenous X-linked loci. Lines with successful transgene insertion were confirmed by Sanger sequencing.

Transcription of X-linked genes was measured by imaging embryos homozygous for the MS2- or PP7-tagged gene and a constitutively expressed *Histone-RFP; MCP-eGFP* (Garcia et al. 2013) or *PCP-eGFP* (Larson et al. 2011) allele.

Live imaging:

Image acquisition:

Sample preparation followed the procedures described in (Bothma et al. 2014, Garcia et al. 2013, Lammers et al. 2020). In brief, embryos were collected, dechorinated with 50% bleach, and mounted between a semipermeable membrane (Lumox film, Starstedt, Germany) and a coverslip while in Halocarbon 27 oil (Sigma). Data collection was

performed using a Zeiss LSM 800 scanning confocal microscope (Zeiss, Jana, Germany). The MCP-eGFP or PCP-eGFP were excited with laser wavelengths of 488 nm, respectively. Data were collected at a 40X objective with oil immersion where the average laser power on the specimen was 7.3 mW and a master gain of 550V. The confocal stack consisted of 21 equidistant slices with an overall z-height of 5.97 µm and an interslice distance of 0.29 µm. The images were acquired at a frame time of 633.02 ms and a pixel dwell time of 1.03 µs. Image sizes were 78 µm x 19.5 µm, a frame size of 1024 pixels x 256 pixels, and a pixel size of 0.08 µm. Data were taken for at least 3 embryos of each sex per genotype, and each embryo was imaged for at least the first 30 minutes of nuclear cycle 14.

Image analysis:

Live-imaging data were analyzed using a custom-written software following the protocols in (Garcia et al. 2013, Lammers et al. 2020). This software, containing MATLAB code, can be found in a public GitHub repository. In brief, this procedure involves nuclear segmentation, segmenting transcription spots based on fluorescence, and calculating the intensity of each MCP-eGFP or PCP-eGFP transcription spot inside a nucleus as a function of time.

Data analysis

To infer bursting parameters from experimental fluorescence traces, we used a compound-state hidden Markov Model described in Lammers et al. 2020 whose code can be found in a public GitHub repository.

All data analysis was done in Python using a Jupyter Notebook with custom code to generate figures. The Jupyter notebook and all data required to run it are available in Supplementary File 1 this Github link .

Quantitative RNA-FISH:

Probe design and hybridization:

Custom Stellaris® FISH Probes were designed against *gt* and *bnb* RNA by utilizing the Stellaris® RNA FISH Probe Designer (Biosearch Technologies, Inc., Petaluma, CA) available online at www.biosearchtech.com/stellarisdesigner (version 4.2). Single-molecule RNA-FISH protocol was followed using the *D. melanogaster* embryo protocol at the Biosearch Technologies website.

Image acquisition:

Embryos were staged at nuclear cycle 14A based on percent membrane invagination during cellularization (< 25%). Data collection was performed using a Zeiss LSM 800 scanning confocal microscope (Zeiss, Jana, Germany). A laser wavelength of 670 nm was used to excite the probe-conjugated fluors. Data were collected at a 63X objective with oil immersion with the laser power on the specimen was set to 5% and a master gain of 650V. The images were acquired at a frame time of 930.91 ms and a pixel dwell time of 1.52 µs. Image sizes were 202.8 µm x 202.8 µm, a frame size of 512 pixels x 512 pixels, and a pixel size of 0.4 µm.

The field of view was adjusted to encompass the entire expression domain of probed patterned genes, and the bounds of the z-stack for each image were determined by when the z-plane no longer detected the probe fluorescent signal.

Full details of probe sequence information can be found in a public Benchling folder. Raw and max intensity projection images can be found in Supplemental File 2.

Image analysis:

Total signal of mRNA with background correction was measured for probed genes using ImageJ. Z-slices of the original image that contained no signal were trimmed from the image before generating a 2D max intensity projection. We followed the Cooper Lab protocol for Quantitation of Total Fluorescence per Cell with Background correction (https://cooperlab.wustl.edu/). In brief, two ROIs were determined in ImageJ: one to measure signal and the other to measure background. We then averaged the mean Integrated Density of the signal (5 separate measurements encompassing the total expression domain) and of the background. The mean background is subtracted from the mean integrated density, and then divided by the area of the signal ROI to obtain the Corrected Integrated Density.

Results

Previous work identified a wide-spread dosage compensation of zygotic transcripts prior to cellularization, where 36 out of 85 X-linked genes showed less than a 1.5-fold excess

of transcript abundance in female embryos relative to their male counterparts (Lott *et al.,* 2011). Many of these early-compensated genes are key developmental regulators, where differences in transcript abundance could pose profound consequences to organismal development. Because these early-compensated genes are regulated before MSL-2, the molecule that mediates canonical dosage compensation, is expressed, we sought to investigate if the early-compensation of these developmental regulators occurred through a transcriptional mechanism independent of MSL-2.

We chose two early-compensated genes (*gt* and *btd*) for further study that are essential for mediating embryonic development and whose mRNA abundance is matched in male and female embryos during the early nuclear cycles. Because not all zygotically-transcribed genes emanating from X are early-compensated, we chose two additional genes (*elav* and *bnb*) with twice as much female mRNA abundant relative to males as a point of comparison in our study. All four of these genes reach maximum transcript abundance during the first half of nuclear cycle 14 (Lott *et al.,* 2011), mitigating any differences due to developmental stages across datasets.

We used CRISPR-Cas9 (Gratz *et al.,* 2015) to insert an array of either MS2 or PP7 stem loop sequences immediately upstream of the translation start codon of the endogenous gene of interest. The rationale behind choosing this insertion site was to position at the stem loops sequences at beginning of the resulting transcript, ensuring a robust reporter signal of when transcription is occurring. The MS2 or PP7 sequences were flanked by the donor and acceptor splice sites from the *hunchback* intron so that

the stem loops would be removed from the mature mRNA to prevent problems with RNA localization (Heinrich *et al.,* 2017) or the translation of the endogenous protein.

We homozygosed the lines containing MS2 and PP7-tagged genes and crossed in a transgene encoding an MCP-GFP (or PCP-GFP) fusion protein that binds transcribed stem loop sequences. The binding of fluorescently conjugated coat protein to these stem loops (Bernardi *et al.,*1972) gives rise to a fluorescent puncta (what we will refer to as "spots" moving forward) in the nucleus (Figure 1B; Garcia *et al.,* 2013) whose fluorescence intensity correlates with the abundance of RNA present at the locus (Garcia et al. 2013). This system offers a spatio-temporal and quantitative characterization of transcript abundance for a gene of interest (Movies 1 & 2).

Figure 1: MS2-MCP and PP7-PCP reporter systems measure transcription rate of X-linked genes in the early *Drosophila melanogaster* embryo A) An example schematic of how the PP7-PCP reporter system works: 24 repeats of the PP7 stem loop sequence (yellow) are flanked by splice donor and acceptor sites from the intron of the *hunchback* gene (gold) were inserted upstream of the target gene's start codon (ATG), represented here by the gene "*buttonhead*". When transcribed, the PP7 form RNA step loops that are subsequently bound by PP7 Coat Protein (orange) conjugated to GFP (green). B) The anterior portion of an embryo expression *PP7-buttonhead* (*PP7-btd*). C) Zoomed-in view of the *PP7-btd* expression domain in a female embryo, made evident by the two transcribing loci in nuclei as opposed to D) the same field of view for *PP7-btd* expression in a male embryo, where there is only one transcribing locus per nucleus.

Embryos with successfully incorporated MS2-MCP or PCP-PP7 reporter systems showed no signs of impaired organismal health and faithfully recapitulated the tagged gene's expression patterns previously reported by FISH (Figure 1B; Wimmer *et al.,* 1996, Tomancak et al. 2002). A key feature of this system that lends itself for studying dosage compensation is the ease in sexing embryos–the fluorescent spots in nuclei serve as a readout for the number of X chromosomes present (embryos with two fluorescent spots within the same nucleus are female, while embryos with one spot are male) (Figure 1C & 1D).

We used laser-scanning confocal microscopy to acquire MCP-GFP (or PCP-GFP) movies of embryos during nc14, the last nuclear cycle before gastrulation. To ensure consistency across fields of view across these high magnification movies, we optimized data collection for patterned genes to capture all nuclei along the AP axis within the same single expression domain (Movies 1 & 2, Supplemental Figure 1). If a gene had a more ubiquitous expression domain within the anterior domain of the embryo, we positioned the anterior pole relative to the field of view consistently across all data collections. To obtain high temporal resolution and optimize signal-to-noise with minimal bleaching, we collected movies so that the acquisition time for each timepoint (or Z-stack) corresponded to intervals of 19.5s. In total, we collected 51 movies (Movies 3-51) with a minimum of three movies of each sex per genotype (see Table 1).

Embryo ID	Gene	Sex	nuclear cycle	Duration (in frames)	Total time	Movie #
M_btd_1	PP7-btd	M	14	159	51.675	Movie 1
F_btd_1	PP7-btd	F	14	172	55.9	Movie 2
M_btd_2	PP7-btd	M	14	142	46.15	Movie 3
M_btd_3	PP7-btd	M	14	162	52.65	Movie 4
M_btd_4	PP7-btd	M	14	125	40.625	Movie 5
M_btd_5	PP7-btd	M	14	141	45.825	Movie 6
M_btd_6	PP7-btd	M	14	183	59.475	Movie 7
M_btd_7	PP7-btd	M	14	99	32.175	Movie 8
M_btd_8	PP7-btd	M	14	110	35.75	Movie 9
M_btd_9	PP7-btd	M	14	94	30.55	Movie 10
F_btd_2	PP7-btd	F	14	122	39.65	Movie 11
F_btd_3	PP7-btd	F	14	194	63.05	Movie 12
F_btd_4	PP7-btd	F	14	208	67.6	Movie 13
F_btd_5	PP7-btd	F	14	123	39.975	Movie 14
F_btd_6	PP7-btd	F	14	176	57.2	Movie 15
F_btd_7	PP7-btd	F	14	166	53.95	Movie 16
F_btd_8	PP7-btd	F	14	173	56.225	Movie 17
F_btd_9	PP7-btd	F	14	119	38.675	Movie 18
M_gt_1	MS2-gt	M	14	119	38.675	Movie 19
M_gt_2	MS2-gt	M	14	148	48.1	Movie 20
M_gt_3	MS2-gt	M	14	125	40.625	Movie 21
M_gt_4	MS2-gt	M	14	114	37.05	Movie 22
F_gt_1	MS2-gt	F	14	111	36.075	Movie 23
F_gt_2	MS2-gt	F	14	143	46.475	Movie 24
F_gt_3	MS2-gt	F	14	147	47.775	Movie 25
F_gt_4	MS2-gt	F	14	139	45.175	Movie 26
M_bnb_1	PP7-bnb	M	14	102	33.15	Movie 27
M_bnb_2	PP7-bnb	M	14	122	39.65	Movie 28
M_bnb_3	PP7-bnb	M	14	122	39.65	Movie 29
F_bnb_1	PP7-bnb	F	14	160	52	Movie 30
F_bnb_2	PP7-bnb	F	14	146	47.45	Movie 31
F_bnb_3	PP7-bnb	F	14	157	51.025	Movie 32
M_elav_1	MS2-elav	M	14	133	43.225	Movie 33
M_elav_2	MS2-elav	M	14	148	48.1	Movie 34
M_elav_3	MS2-elav	M	14	128	41.6	Movie 35
F_elav_1	MS2-elav	F	14	139	45.175	Movie 36
F_elav_2	MS2-elav	F	14	159	51.675	Movie 37
F_elav_3	MS2-elav	F	14	141	45.825	Movie 38
M13_btd_1	PP7-btd	M	13	33	10.725	Movie 39
M13_btd_2	PP7-btd	M	13	31	10.075	Movie 40
M13_btd_3	PP7-btd	M	13	25	8.125	Movie 41
F13_btd_1	PP7-btd	F	13	26	8.45	Movie 42
F13_btd_2	PP7-btd	F	13	23	7.475	Movie 43
F13_btd_3	PP7-btd	F	13	23	7.475	Movie 44
M13_bnb_1	PP7-bnb	M	13	38	12.35	Movie 45
M13_bnb_2	PP7-bnb	M	13	25	8.125	Movie 46
M13_bnb_3	PP7-bnb	M	13	29	9.425	Movie 47
F13_bnb_1	PP7-bnb	F	13	50	16.25	Movie 48
F13_bnb_2	PP7-bnb	F	13	44	14.3	Movie 49
F13_bnb_3	PP7-bnb	F	13	32	10.4	Movie 50

Table 1: MS2 or PP7 live-imaging data collected in this study

We used a custom image analysis pipeline (Garcia et al. 2013, Lammers et al. 2020) to identify nuclei and extract fluorescent intensity measurements for actively transcribing X-linked loci in embryos of both sexes. A representative example of the resulting data is shown in Figure 2.

No hyper-transcription of male X in dosage compensated genes

We compared the average fluorescence intensity (which we expect to be proportional to polymerase density on transcribing loci) of detected transcription foci from male and female X chromosomes across time during mitotic cycle 14 for both *btd* and *gt* (Figure 2A). For *btd* they are nearly identical, and for *gt*, the differences both balances out over time (with slightly higher transcription from male X's early in cycle 14 and slightly higher transcription from female X's later in cycle 14). As it is possible to increase transcriptional output even with identical polymerase density on transcribing loci by increasing the fraction of loci actively transcribing, we also looked at the number of transcribing loci as a function of time in male and female embryos (Figure 2B), and, as expected, observed them to be in approximately a 2:1 ratio between females and males. These results are inconsistent with early dosage compensation of *btd* and *gt* being achieved via hyper-transcription of the male X.

Figure 2: Transcription rate of the early dosage compensated *PP7-btd* and *MS2-gt* genes is the same in male and female embryos

A) Average distributions of fluorescent spot intensity over time (in frames, where "1" is the first instance of transcription of the locus during nuclear cycle 14) for all female

(orange) and male (dark cyan) *PP7-btd* (N=9 embryos of each sex) and *MS2-gt* (N=4 of each sex) embryos. The dashed, dark orange line represents double the average female fluorescent spot intensity for every given timepoint. B) The distribution of fluorescent spot intensities plotted over time for the dosage compensated *MS2-gt* (N=4 embryos of each sex) with total spot intensity histograms on the right. B) The number of transcribing *PP7-btd* and *MS2-gt* loci throughout nuclear cycle 14. The dashed orange line represents half of the transcribing female loci.

We made similar comparisons between average fluorescence and number of transcribing loci in the two non-compensated loci bnb and elav. These show more variation between sexes than two dosage compensated genes, with bnb generally higher in males, and elav higher in females (Figure 3).

Figure 3: Transcription rate of *PP7-bnb* and *MS2-elav* is does not result in dosage compensation

A) Averages for male (dark cyan) and female (orange) *PP7-bnb* and *MS2-elav* fluorescent spot intensities plotted over nuclear cycle 14. The dashed, dark orange line represents double the average female fluorescent spot intensity for every given timepoint. B) The number of transcribing *PP7-bnb* and *MS2-elav* loci throughout nuclear cycle 14. The dashed orange line represents half of the transcribing female loci.

Discussion

Our tailoring of quantitative live-imaging methods to examine early embryonic dosage compensation in *Drosophila melanogaster* were motivated by the hypothesis that the equalizing of mRNA abundance between sexes in the absence of MSL-2 mediated by regulation of transcription rate at X-linked loci.

Instead, what our studies revealed was a post-transcriptional mechanism for regulating early dosage compensation of two key developmental regulators, *btd* and *gt.* These findings represent a broadening of our understanding of different ways in which the sex chromosome dosage imbalance is mitigated during early embryogenesis. Our findings offer a more dynamic way of understanding how mRNA abundance is regulated across developmental stages. Importantly, this presents a shift in our understanding of how mRNA abundance is regulated considering the decades of research whose findings posited that dosage compensation is almost exclusively a transcriptionally regulated process.

Sex lethal (Sxl), and RNA-binding protein that inhibits dosage compensation in females, may play a role in regulating the abundance of X-linked mRNAs during early embryogenesis. The regulation of X-linked *runt* abundance by Sxl is the only documented observation of an MSL-2-independent, post-transcriptional regulation of dosage compensation prior to our study (Gergen 1987, Bernstein and Cline 1994). It is possible that because the two molecules regulate each other's expression (Kramer et al. 1999, Torres et al. 2009), that observation of post-transcriptional dosage

compensation by Sxl is gene-specific and therefore inapplicable to the widespread phenomenon we observe during early embryogenesis (Lott et al. 2011).

Considering our findings, the observed enrichment of predicted Sxl binding sites (poly-U tracts) in the 5' and 3' UTRs of many X-linked genes (Kelley et al. 1995) may point to one mechanism for post-transcriptionally regulating dosage compensation. There is no direct correlation between genes that are early dosage compensated and their predicted regulation by Sxl–not all genes that are early dosage compensated are predicted to be Sxl targets, and not all predicted Sxl targets are early dosage compensation. There may however be a subset of early dosage-compensated genes whose abundance may be regulated by Sxl, a hypothesis worth exploring in future studies.

It is formally possible that regulation of transcriptional elongation may mediate early dosage compensation of *btd* and *gt*. Because the MS2 and PP7 stem loop sequences in our study are inserted immediately upstream of the translation start codon and flanked by splice donor and acceptor sites from the *hb* intron, our findings speak only to the regulation of transcription initiation. However, a recent study using MS2 and PP7 reporter systems demonstrated a concerted regulation of transcription initiation as opposed to a highly variable regulation of elongation between nuclei (Liu et al. 2020). These findings suggest that elongation is not the major contributor to transcriptional regulation, though the role of elongation during early dosage compensation using these tools warrants further study.

While the primary goal of this study was to study dosage compensation, our measurements of transcription rate at endogenous loci represent a significant advance for *in vivo* studies of mechanisms of gene regulation in the *D. melanogaster* embryo. Our use of our reporter at an X-linked loci for sexing embryos also provides a straightforward control for detecting differences in the regulation of gene expression between male and female embryos.

We hope that our data, as well as the reagents generated for the purposes of our study, can help address other open questions about gene regulation in the early *D. melanogaster* embryo. The reagents generated can be used for protein colocalization studies or can be crossed mutant alleles of interest to assess the contribution of a particular molecule in the regulation of our tagged genes. Overall, we are eager to learn how the data and reagents generated in our discovery of a post-transcriptional form of early dosage compensation make possible future learnings that deepen the community's understanding of regulating gene expression during development.

Supporting Information

Supplementary Figure 1: Transcription rate of *PP7-btd* and *MS2-gt* is the same in male and female embryos

A) Distributions of fluorescent spot intensity over time (in frames, where "1" is the the first instance of transcription of the locus during nuclear cycle 14) for all female (orange) and male (dark cyan) embryos (N=9 embryos of each sex) with total spot intensity

391 histograms on the right. B) The distribution of fluorescent spot intensities plotted over
392 time for the dosage compensated *MS2-gt* (N=4 embryos of each sex) with total spot
393 intensity histograms on the right. B&C) The distribution of fluorescent spot intensities
394 plotted over time for *PP7-bnb* and *MS2-elav*, genes that are not early dosage
395 compensated (N=3 embryos of each sex for each genotype) with total spot intensity
396 histograms on the right.
397
398 **Supplementary Figure 2: Validation of early dosage compensation phenotype by**
399 **quantitative FISH** A) A maximum intensity projection of the anterior portion of a wild
400 type male embryo at early nc14 probed for *gt* (an early dosage compensated gene)
401 RNA and B) a female embryo probed for *bnb* (an X-linked gene that is not early dosage
402 compensated) RNA. Embryos were sexed by determining the number of large puncta
403 were present within nuclei, which are dark and circular in appearance. C & D)
404 Quantification of total probe signal for each probe in individual embryos, where the
405 signal intensity was averaged across the expression domain with background
406 subtraction.
407
408 **Supplemental Figure 3: Transcription rate for *PP7-btd* and *PP7-bnb* are the same**
409 **in male and female embryos at nuclear cycle 13** A) The total distribution of
410 fluorescent spot intensities and the same data plotted over the course of nuclear cycle
411 13 for *PP7-btd* (N=3 embryos for each sex). B) The total distribution of fluorescent spot
412 intensities and the same data plotted over the course of nuclear cycle 13 for *PP7-bnb*
413 (N=3 embryos for each sex).

Supplemental Figure 4: Total distribution of spot intensities of *MS2-gt, MS2-elav*, and *PP7-bnb* A) Total distributions of fluorescent spot intensity for all female (orange) and male (dark cyan) *MS2-gt* embryos (N=4 embryos for each sex) and the same data plotted for individual embryos by sex. We also plotted data for *MS2-elav* in B) and *PP7-bnb* in C) in the same manner (N=3 embryos for each sex per genotype).

Supplementary Figure 5: Transcription rate of *PP7-btd* varies along the Dorsal-Ventral axis of the developing embryo A) Distribution of fluorescent intensity of *PP7-btd* spots in individual male and female embryos. B) Variation in the width of the *PP7-btd* expression domain along the DV axis, where the dorsal (39% of the field of view) expression domain correlates with spots of weaker fluorescence intensity (indicated by the green color that matches one of the individual histograms of a male embryo in A). An embryo whose recorded *PP7-btd* expression is more ventral (52% field of view) has a wider distribution of spot fluorescent intensities. C) Distribution of fluorescent spot intensities of individual embryos matched by FOV, and therefore, DV position. D) Average particle intensities plotted over time for two male and female embryos on different positions on the DV axis.

Acknowledgments:

We thank Hernan Garcia for pioneering techniques for quantitative imaging of live embryos and for project insight; Nicholas Lammers for help with computational analysis; Gabriella Martini for generating the *MS2-gt* fly line; Barbara Meyer, Nicholas Ingolia,

and Doris Bachtrog for helpful comments; Michael Stadler and members of the Eisen lab for helpful comments and project insight.

References:

Beadle LR, Love LC, Shapovalova Y, Artemev A, Rattray M, Ashe HL. Modelling global mRNA dynamics during *Drosophila* embryogenesis reveals a relationship between mRNA degradation and P-bodies. bioRxiv:484585 [Preprint]. 2022 [cited 2022 April 20] Available from: https://doi.org/10.1101/2022.03.17.484585.

Belote JM, Lucchesi JC. MALE-SPECIFIC LETHAL MUTATIONS OF DROSOPHILA MELANOGASTER. Genetics [Internet]. 1980;96(1):165–86. Available from: http://dx.doi.org/10.1093/genetics/96.1.165

Bernardi A, Spahr PF. Nucleotide sequence at the binding site for coat protein on RNA of bacteriophage R17. Proc Natl Acad Sci U S A [Internet]. 1972;69(10):3033–7. Available from: http://dx.doi.org/10.1073/pnas.69.10.3033).

Bernstein M, Cline TW. Differential effects of Sex-lethal mutations on dosage compensation early in Drosophila development. Genetics [Internet]. 1994;136(3):1051–61. Available from: http://dx.doi.org/10.1093/genetics/136.3.1051

Bothma JP, Garcia HG, Esposito E, Schlissel G, Gregor T, Levine M. Dynamic regulation of eve stripe 2 expression reveals transcriptional bursts in living Drosophila

460 embryos. Proc Natl Acad Sci U S A [Internet]. 2014;111(29):10598–603. Available from:
461 http://dx.doi.org/10.1073/pnas.1410022111
462
463 Garcia HG, Tikhonov M, Lin A, Gregor T. Quantitative imaging of transcription in living
464 Drosophila embryos links polymerase activity to patterning. Curr Biol [Internet].
465 2013;23(21):2140–5. Available from: http://dx.doi.org/10.1016/j.cub.2013.08.054
466
467 Gelbart ME, Larschan E, Peng S, Park PJ, Kuroda MI. Drosophila MSL complex
468 globally acetylates H4K16 on the male X chromosome for dosage compensation. Nat
469 Struct Mol Biol [Internet]. 2009;16(8):825–32. Available from:
470 http://dx.doi.org/10.1038/nsmb.1644
471
472 Gergen JP. Dosage compensation in Drosophila: Evidence that daughterless and sex-lethal
473 control X chromosome activity at the blastoderm stage of embryogenesis. Genetics [Internet].
474 1987;117(3):477–85. Available from: http://dx.doi.org/10.1093/genetics/117.3.477
475
476 Gratz SJ, Rubinstein CD, Harrison MM, Wildonger J, O'Connor-Giles KM. CRISPR-
477 Cas9 genome editing in Drosophila. Curr Protoc Mol Biol [Internet]. 2015;111(1):31.2.1-
478 31.2.20. Available from: http://dx.doi.org/10.1002/0471142727.mb3102s111
479
480 Heinrich S, Sidler CL, Azzalin CM, Weis K. Stem–loop RNA labeling can affect nuclear
481 and cytoplasmic mRNA processing. RNA [Internet]. 2017;23(2):134–41. Available from:
482 http://dx.doi.org/10.1261/rna.057786.116

Hilfiker A, Hilfiker-Kleiner D, Pannuti A, Lucchesi JC. mof, a putative acetyl transferase gene related to the Tip60 and MOZ human genes and to the SAS genes of yeast, is required for dosage compensation in Drosophila. EMBO J [Internet]. 1997;16(8):2054–60. Available from: http://dx.doi.org/10.1093/emboj/16.8.2054

Kane NS, Vora M, Varre KJ, Padgett RW. Efficient screening of CRISPR/Cas9-induced events in Drosophila using a co-CRISPR strategy. G3 (Bethesda) [Internet]. 2017;7(1):87–93. Available from: http://dx.doi.org/10.1534/g3.116.036723

Kelley RL, Solovyeva I, Lyman LM, Richman R, Solovyev V, Kuroda MI. Expression of msl-2 causes assembly of dosage compensation regulators on the X chromosomes and female lethality in Drosophila. Cell [Internet]. 1995;81(6):867–77. Available from: http://dx.doi.org/10.1016/0092-8674(95)90007-1

Kramer SG, Jinks TM, Schedl P, Gergen JP. Direct activation of Sex-lethal transcription by the Drosophila runt protein. Development [Internet]. 1999;126(1):191–200. Available from: http://dx.doi.org/10.1242/dev.126.1.191

Kuroda MI, Hilfiker A, Lucchesi JC. Dosage compensation in Drosophila-a model for the coordinate regulation of transcription. Genetics [Internet]. 2016;204(2):435–50. Available from: http://dx.doi.org/10.1534/genetics.115.185108

506 Lammers NC, Galstyan V, Reimer A, Medin SA, Wiggins CH, Garcia HG. Multimodal
507 transcriptional control of pattern formation in embryonic development. Proc Natl Acad
508 Sci U S A [Internet]. 2020;117(2):836–47. Available from:
509 http://dx.doi.org/10.1073/pnas.1912500117
510
511 Larson DR, Zenklusen D, Wu B, Chao JA, Singer RH. Real-time observation of transcription
512 initiation and elongation on an endogenous yeast gene. Science [Internet]. 2011;332(6028):475–
513 8. Available from: http://dx.doi.org/10.1126/science.1202142
514
515 Liu J, Hansen, Eck E, Kim YJ, Turner M, Alamos S, Garcia HG. Real-time single-cell
516 characterization of the eukaryotic transcription cycle reveals correlations between RNA
517 initiation, elongation, and cleavage. bioRxiv:273474 [Preprint]. 2020 [cited 2022 April
518 20]. Available from: https://doi.org/10.1101/2020/08.29.273474.
519
520 Lott SE, Villalta JE, Schroth GP, Luo S, Tonkin LA, Eisen MB. Noncanonical
521 compensation of zygotic X transcription in early Drosophila melanogaster development
522 revealed through single-embryo RNA-seq. PLoS Biol [Internet]. 2011;9(2):e1000590.
523 Available from: http://dx.doi.org/10.1371/journal.pbio.1000590
524
525 Lucchesi JC, Skripsky T. The link between dosage compensation and sex differentiation
526 in Drosophila melanogaster. Chromosoma [Internet]. 1981;82(2):217–27. Available
527 from: http://dx.doi.org/10.1007/bf00286106
528

529 Meller VH, Rattner BP. The roX genes encode redundant male-specific lethal transcripts
530 required for targeting of the MSL complex. EMBO J [Internet]. 2002;21(5):1084–91.
531 Available from: http://dx.doi.org/10.1093/emboj/21.5.1084
532
533 Port F, Bullock SL. Augmenting CRISPR applications in Drosophila with tRNA-flanked
534 sgRNAs. Nat Methods [Internet]. 2016;13(10):852–4. Available from:
535 http://dx.doi.org/10.1038/nmeth.3972
536
537 Pritchard DK, Schubiger G. Activation of transcription in Drosophila embryos is a
538 gradual process mediated by the nucleocytoplasmic ratio. Genes Dev [Internet].
539 1996;10(9):1131–42. Available from: http://dx.doi.org/10.1101/gad.10.9.1131
540
541 Smith ER, Allis CD, Lucchesi JC. Linking global histone acetylation to the transcription
542 enhancement of X-chromosomal genes in Drosophila males. J Biol Chem [Internet].
543 2001;276(34):31483–6. Available from: http://dx.doi.org/10.1074/jbc.c100351200
544
545 Smith ER, Pannuti A, Gu W, Steurnagel A, Cook RG, Allis CD, et al. The Drosophila
546 MSL complex acetylates histone H4 at lysine 16, a chromatin modification linked to
547 dosage compensation. Mol Cell Biol [Internet]. 2000;20(1):312–8. Available from:
548 http://dx.doi.org/10.1128/mcb.20.1.312-318.2000
549
550 Tomancak P, Beaton A, Weiszmann R, Kwan E, Shu S, Lewis SE, et al. Systematic
551 determination of patterns of gene expression during Drosophila embryogenesis.

552 Genome Biol [Internet]. 2002;3(12):RESEARCH0088. Available from:
553 http://dx.doi.org/10.1186/gb-2002-3-12-research0088
554
555 Torres M, Sánchez L. The segmentation gene runt is needed to activate Sex-lethal, a gene that
556 controls sex determination and dosage compensation in Drosophila. Genet Res. 1992;59(3):189–
557 98.
558
559 Wimmer EA, Frommer G, Purnell BA, Jäckle H. buttonhead and D-Sp1: a novel
560 Drosophila gene pair. Mech Dev [Internet]. 1996;59(1):53–62. Available from:
561 http://dx.doi.org/10.1016/0925-4773(96)00575-8
562
563
564 Zoller B, Little SC, Gregor T. Diverse spatial expression patterns emerge from unified
565 kinetics of transcriptional bursting. Cell [Internet]. 2018;175(3):835-847.e25. Available
566 from: http://dx.doi.org/10.1016/j.cell.2018.09.056
567
568
569

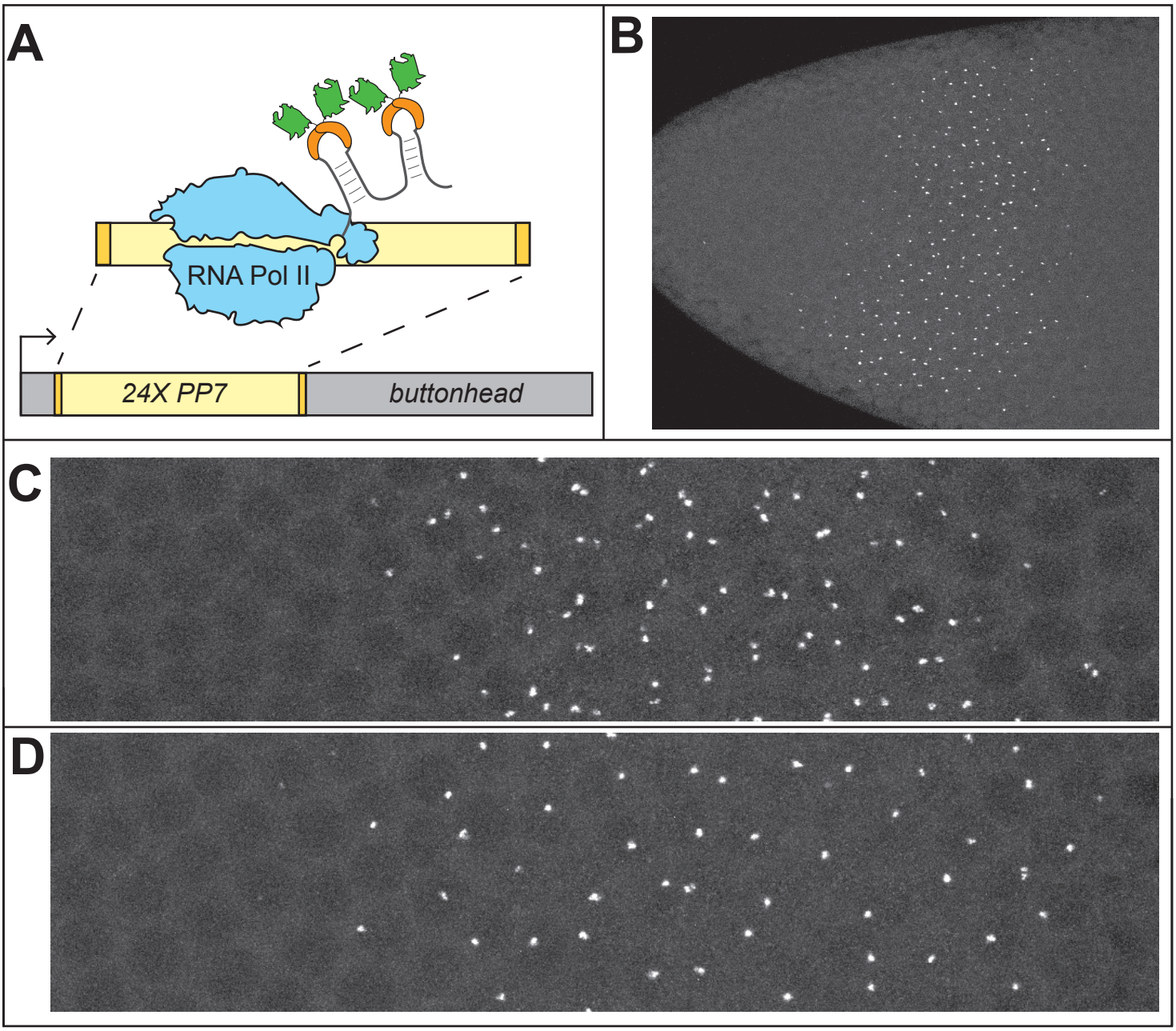

A

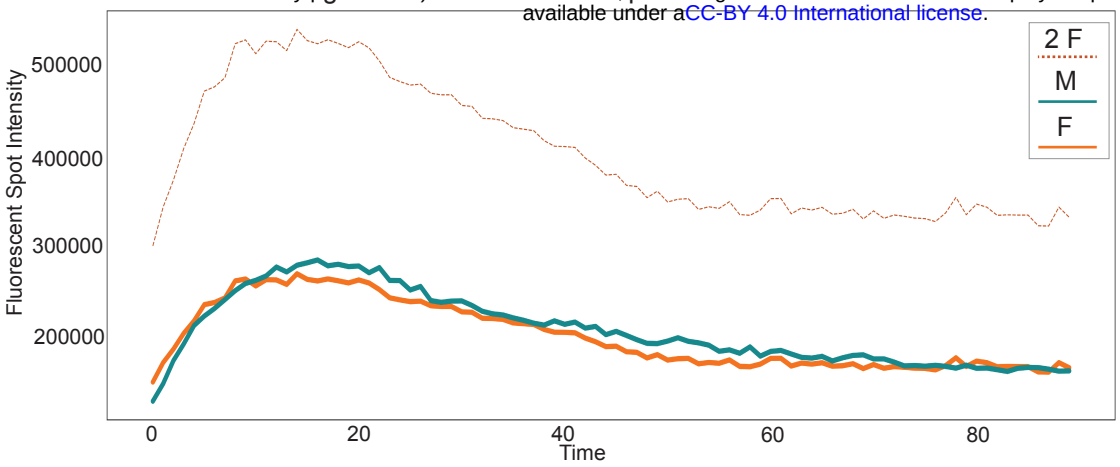

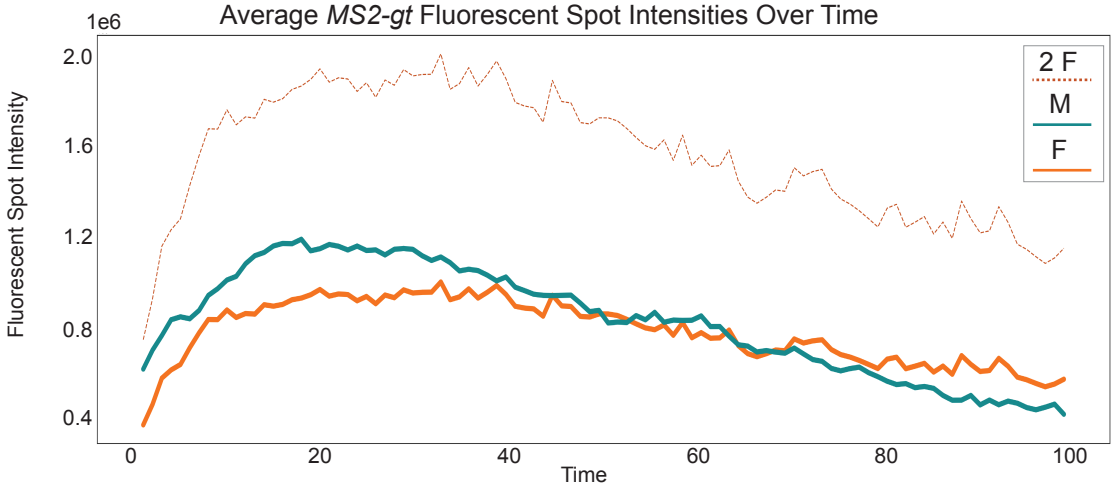

B

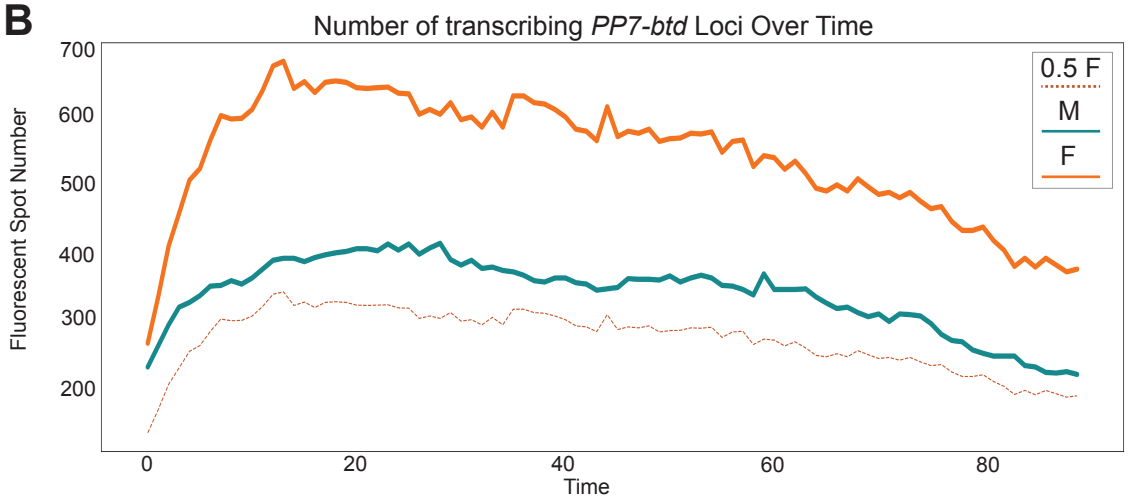

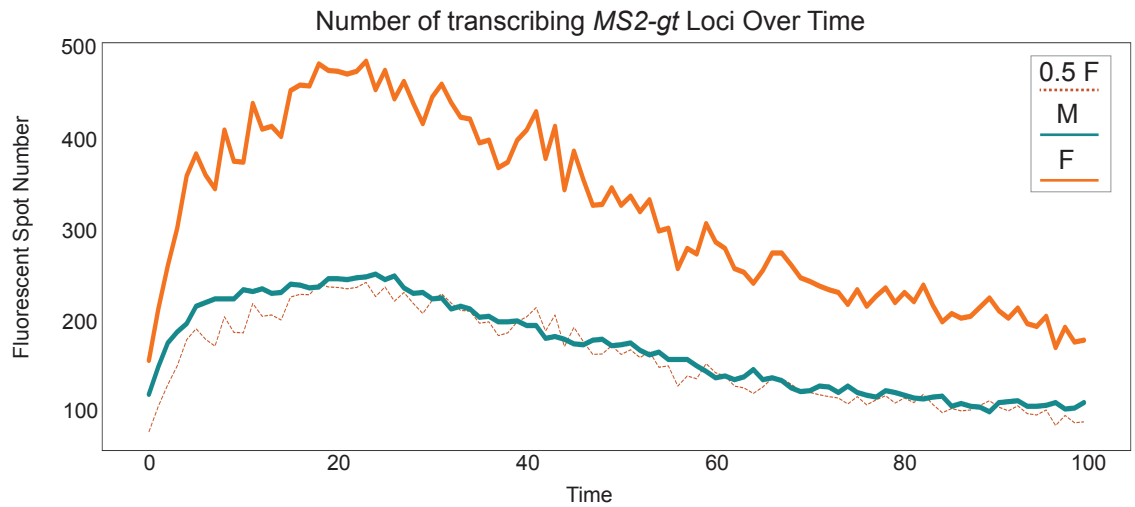

A

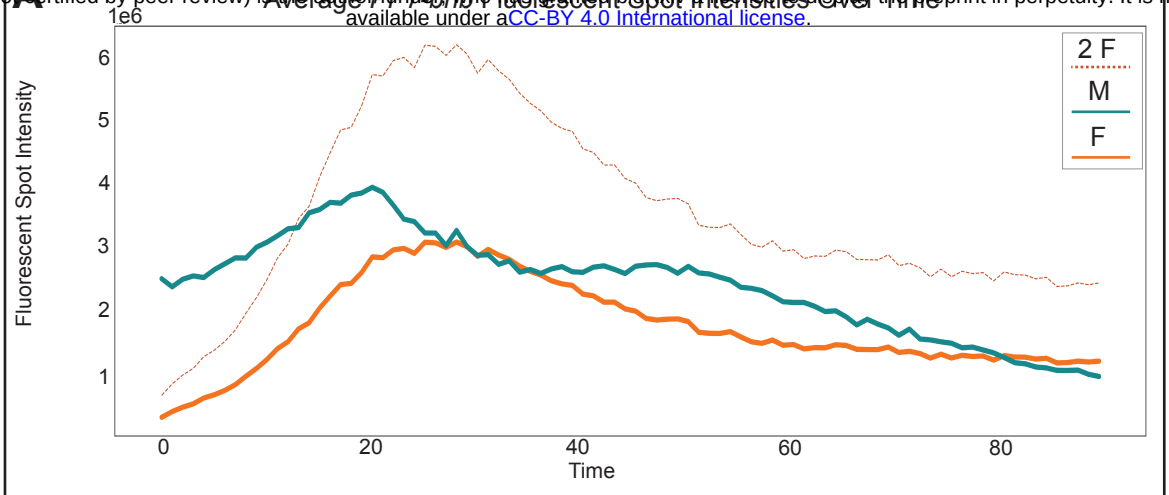

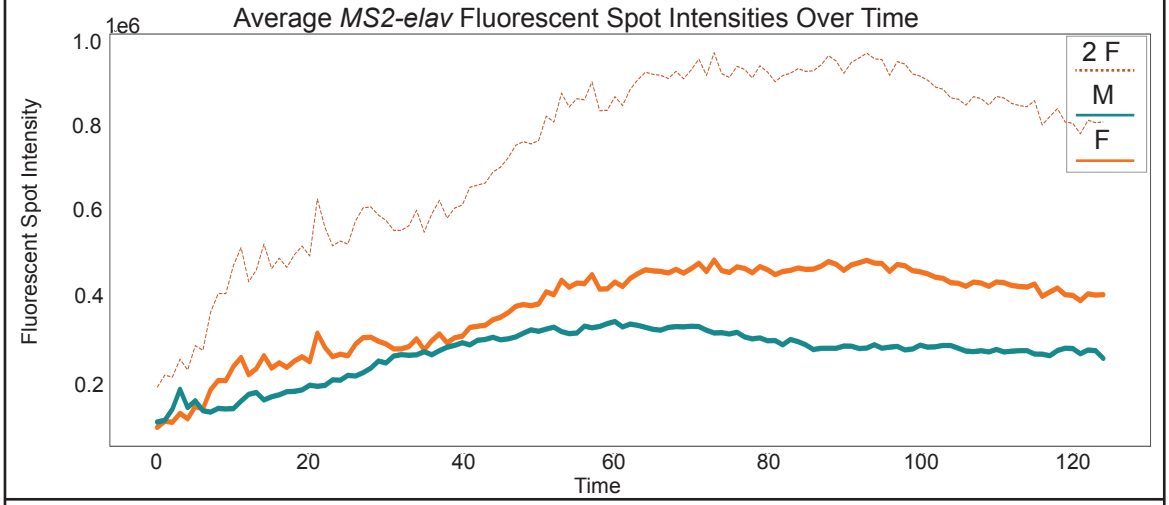

B